Research Square

Preprints are preliminary reports that have not undergone peer review.
They should not be considered conclusive, used to inform clinical practice,
or referenced by the media as validated information.

Resting-state fMRI correlates of self-balancing robot-assisted lower-limb rehabilitation after stroke: a pilot randomized controlled neuroimaging study

Yanzheng Zhang
Shanghai Hebin Rehabilitation Hospital
Qijin Zhai
Huai'an Clinical Medical College of Jiangsu University
Yang Wang
Hanzhong Central Hospital
Zhichao Liu
Huashan Hospital
Limin Sun
Huashan Hospital
Yulin Li
Huashan Hospital
Yuanyuan Chu
Shanghai Hebin Rehabilitation Hospital
Zhe Li
Shanghai Hebin Rehabilitation Hospital
Liwang Deng
Shanghai Hebin Rehabilitation Hospital
Bin Su
Jiangsu Medical College
Wei Sun
The First People's Hospital of Chenzhou
Yanjie Hu
Huashan Hospital
Ling Ding
Shanghai Fifth People's Hospital
Hewei Wang
wanghew@fudan.edu.cn

Huashan Hospital

Research Article

Keywords: stroke, robotic rehabilitation, lower limb, balance, resting-state fMRI, ALFF, interhemispheric correlation, functional connectivity

Posted Date: September 25th, 2026

DOI: https://doi.org/10.21203/rs.3.rs-10514032/v1

License: This work is licensed under a Creative Commons Attribution 4.0 International License. Read Full License

Additional Declarations: No competing interests reported.

Abstract

Background

Lower-limb weakness and poor balance are major barriers to independent walking after stroke. Self-balancing robot-assisted training permits supported upright practice, repeated weight shifting and task-oriented lower-limb loading, but its training-related neural correlates remain unclear.

Methods

In this pilot randomized controlled neuroimaging study, 24 patients with subcortical stroke received 4 weeks of REX-assisted training plus conventional rehabilitation or dose-matched active upright lower-limb training plus conventional rehabilitation (n = 12 per group). The Berg Balance Scale (BBS) was the primary clinical outcome, the Fugl-Meyer Assessment of the Lower Extremity (FMA-LE) was the key secondary outcome, and the Postural Assessment Scale for Stroke (PASS) and Functional Ambulation Category (FAC) were exploratory outcomes. Resting-state functional MRI was acquired before and after treatment; 20 participants were retained for imaging analyses (REX, n = 11; control, n = 9). Group-by-time analyses examined amplitude of low-frequency fluctuations (ALFF), affected-side precentral-gyrus seed-based functional connectivity (FC), and interhemispheric correlation (IHC); local and global correlation measures were exploratory.

Results

Baseline-adjusted analyses favored REX for post-intervention BBS scores (adjusted difference, 12.75; 95% CI, 1.45–24.04; P = 0.029) and FMA-LE scores (adjusted difference, 7.19; 95% CI, 3.71–10.67; P < 0.001). FAC was also favorable in an exploratory analysis, whereas PASS did not show a statistically definitive between-group difference. Group-by-time effects were observed in ALFF, seed-based FC, and IHC analyses, involving the affected-side precuneus, non-lesioned-side association cortices, the affected-side precentral–middle temporal connectivity, and bilateral precuneus/posterior cingulate homotopic coordination. Local and global correlation interactions were not significant.

Conclusion

Four weeks of REX-assisted lower-limb rehabilitation was associated with favorable pilot clinical outcomes and selective resting-state fMRI changes involving posterior-midline, visual-association, frontal-control, and motor-association systems. These findings represent candidate training-related neural correlates and require confirmation in larger randomized studies.

Trial registration:

Chinese Clinical Trial Registry, ChiCTR2300079122; (registered on 26 December 2023, https://www.chictr.org.cn/)

Introduction

Stroke commonly leaves patients with lower-limb weakness and poor balance, both of which limit independent walking [1]. For patients who cannot walk independently, rehabilitation must provide frequent upright practice without compromising safety or placing excessive demands on therapists [2, 3]. Early improvement also reflects both spontaneous recovery and experience-dependent adaptation [4]. Therefore, the type and amount of practice remain important in patients with marked disability [5].

Robot-assisted gait and lower-limb training can increase the dose and consistency of supported practice, but the clinical effects are not uniform across trials [6]. Treadmill robots, end-effector systems, wearable exoskeletons and self-balancing devices provide different mechanical assistance and sensory input [7]. Clinical findings for treadmill-based robotic orthoses such as the Lokomat have also been heterogeneous, potentially reflecting differences in patient selection, training protocols, and comparator interventions [8]. In subacute stroke, reported effects also vary with the timing and content of training [9, 10]. A recent meta-analysis reached a similar conclusion for lower-limb robotic training [11]. Overground exoskeleton studies likewise differ in patient stage, device design, training dose and active comparator [12].

REX (WuXi MaxRex Robotic Exoskeleton Ltd., Wuxi, China) is a self-balancing exoskeleton that permits supported upright stance, repeated weight shifting, active loading of the paretic limb, stepping-related practice and continuous visual-proprioceptive feedback [3]. These training demands differ from passive standing and are only partly reproduced by conventional upright exercise [13]. Other overground robotic devices have shown balance-related benefits in subacute stroke, although their assistance strategies are not identical to those of REX [3, 14]. Thus, the therapeutic exposure should be described directly rather than treating all exoskeletons as interchangeable [15]. An earlier independent REX randomized trial reported favorable balance-related outcomes after 4 weeks, but that cohort did not undergo neuroimaging [3].

The neural effects of upright robotic training are unlikely to be confined to primary motor cortex. Post-stroke recovery may involve distributed motor, postural, visuospatial, sensory-integration and interhemispheric systems [16]. Resting-state fMRI is useful in this population because it does not require patients with severe impairment to perform a reliable task in the scanner [17]. Longitudinal stroke studies and early robot-assisted gait studies suggest that resting-state measures can track training-related functional changes, although randomized imaging studies with active controls remain limited [18, 19].

Resting-state changes after stroke do not show a uniform direction or spatial pattern across longitudinal studies [20]. For this reason, we did not formulate a narrow regional hypothesis from the final maps. Resting-state measures are sensitive to motor learning, but such changes should be regarded as candidate correlates rather than direct evidence of recovery mechanisms [21]. Moreover, recent post-walking resting-state studies suggest that the timing of fMRI acquisition relative to motor practice may

influence observed network changes [22]. Interhemispheric motor-cortical communication has been associated with walking after stroke, but this does not establish an effect of robotic training [23]. Fugl-Meyer Assessment of the lower extremity (FMA-LE) was used to quantify lower-extremity motor impairment [24], and its clinical interpretation depends on the population studied [25]. Functional Ambulation Category (FAC) was used to describe the level of ambulatory assistance [26]. We therefore conducted an independent, parallel-group pilot randomized neuroimaging trial of REX-assisted lower-limb rehabilitation after subcortical stroke. Change in Berg Balance Scale (BBS) was the prespecified primary clinical outcome, and FMA-LE was the key secondary outcome. The Postural Assessment Scale for Stroke (PASS) and FAC were exploratory. The formal imaging analyses included amplitude of low-frequency fluctuations (ALFF), seed-based functional connectivity (FC), and interhemispheric correlation (IHC); local correlation (LCOR) and global correlation (GCOR) were supplementary exploratory measures. We examined whether REX was associated with candidate neural correlates in distributed networks.

Materials and Methods

Study Design and Participants

This was a parallel two-arm pilot randomized controlled neuroimaging study with a 4-week intervention period. Participants were recruited at Shanghai Hebin Rehabilitation Hospital between 26 December 2023 and 25 December 2024. Twenty-four patients with subcortical stroke were included in the randomized clinical sample and assigned to the REX group or control group in a 1:1 ratio (Fig. 1). The study was approved by the Ethics Committee of Shanghai Hebin Rehabilitation Hospital (HBRH-MEC2023004) and registered in the Chinese Clinical Trial Registry (ChiCTR2300079122). Written informed consent was obtained from all participants or their legal representatives. The report follows CONSORT 2010 statement [27].

Inclusion criteria were: unilateral hemiparesis after stroke diagnosed according to the 2019 revised Chinese diagnostic criteria for cerebrovascular diseases and confirmed by cranial CT or MRI; first-ever subcortical ischemic or hemorrhagic stroke 2 weeks to 6 months previously; age 18–85 years; Brunnstrom Recovery Stage IV or lower in the paretic lower limb; lower-limb muscle tone no greater than grade 2 on the Modified Ashworth Scale; stable vital signs and neurological status; and no severe cognitive impairment and sufficient ability to understand and follow the training instructions (Montreal Cognitive Assessment score ≥ 16).

Exclusion criteria were: severe arthritis or other serious musculoskeletal disease; severe joint-range limitation that precluded protocol training; severe osteoporosis identified on clinical bone-density assessment; skin injury or infection at device contact sites; orthostatic hypotension, lower-limb deep-vein thrombosis, unstable hypertension, or serious cardiovascular or cardiopulmonary disease precluding exercise; clinically significant speech, attention, hearing, visual (including hemineglect or hemianopia), intellectual, psychiatric, or cognitive impairment; a history of other organic brain disease, neurological or psychiatric disorder, substance misuse, or alcohol misuse; severe cardiac, pulmonary, hepatic, or renal failure; pain with a visual analogue scale score > 4; non-MRI-compatible implanted devices or metallic

foreign bodies; claustrophobia or another MRI contraindication; cranial defect or previous cranioplasty; inability to complete treatment or assessments or poor anticipated adherence; participation in another clinical trial; or another condition judged by the investigators to make participation unsuitable.

Randomization and Blinding

Independent researchers who were not involved in participant recruitment, intervention delivery, or outcome assessment generated the computer-based random-number sequence for 1:1 allocation and prepared and held the sequentially numbered, opaque, sealed envelopes. Envelopes were opened only after completion of baseline assessment and enrolment. Because the robot-assisted intervention was visible and required therapist supervision, participants and treating therapists could not be blinded. All clinical outcomes were assessed by an independent therapist who was blinded to group allocation and was not involved in intervention delivery. Imaging preprocessing and second-level statistical analyses were performed according to a predefined group-by-time framework.

As an exploratory neuroimaging pilot, the study was not powered for definitive imaging efficacy hypotheses. The planned sample of 24 participants (12 per group) was selected pragmatically, informed by the scale of our previous REX pilot trial[3], to assess feasibility, safety, clinical effect-size estimates, and the quality of longitudinal rs-fMRI data for planning a larger definitive trial.

Interventions

Both groups received a standardized conventional rehabilitation program throughout the 4-week treatment period. Conventional rehabilitation included physical therapy, transfer training, sitting and standing balance training, lower-limb strengthening, aerobic exercise as tolerated, occupational therapy and traditional Chinese rehabilitation when clinically indicated. Therapists in both groups had more than 5 years of neurological rehabilitation experience and completed standardized protocol training before the study.

The REX group received conventional rehabilitation plus self-balancing exoskeleton robot-assisted lower-limb training. The REX protocol was a structured task-oriented program emphasizing upright postural control, active weight transfer, visual-proprioceptive feedback and lower-limb loading. Each 60-minute session consisted of three modules: standing balance and reaching tasks in the REX device (approximately 20 minutes), elastic-band resisted upper-limb diagonal tasks performed during supported standing to increase trunk and postural-control demand (approximately 15 minutes), and lower-limb functional training including paretic-limb loading, lateral stepping, repeated unilateral stepping, squatting, alternating forward/backward stepping, robot-assisted sit-to-stand transfer and stair-related practice (approximately 25 minutes).

The control group received conventional rehabilitation plus dose-matched standing-bed-based lower-limb training. Importantly, the control intervention was not passive standing alone. Participants trained in upright standing on the standing bed and performed therapist-supervised tasks designed to match time and therapist attention, including multi-height and multidirectional reaching/operational tasks during

supported standing and paretic-limb loading practice by lifting the non-paretic lower limb while maintaining the standing position. The control program was therefore designed as an active upright-training comparator rather than a no-treatment or passive-standing condition.

Both additional interventions were delivered for 60 minutes per session, once daily, 5 days per week for 4 consecutive weeks, for a planned total of 20 sessions. Training intensity was adjusted according to fatigue, cardiovascular response, balance safety and therapist judgment. Adherence to the allocated intervention was good: all 24 participants completed the 4-week intervention and pre- and post-intervention clinical assessments. No adverse events occurred during the intervention period.

Clinical Outcomes

Clinical outcomes were analyzed in all randomized participants with available pre- and post-intervention assessments. The primary between-group analysis used analysis of covariance (ANCOVA), with the post-intervention score as the dependent variable, treatment group as the fixed effect, and the corresponding baseline score as a covariate. BBS was the prespecified primary clinical outcome; FMA-LE was the key secondary outcome, whereas PASS and FAC were exploratory outcomes. ANCOVA assumptions were evaluated using residual diagnostics (Shapiro-Wilk test, Breusch-Pagan test, group-by-baseline interaction, and Cook's distance); heteroscedasticity-robust HC3 standard errors were examined as a sensitivity analysis. Because FAC is an ordinal scale, its linear ANCOVA was interpreted as exploratory and was complemented by an adjusted cumulative-logit model of post-intervention FAC. All clinical P values were two-sided and nominal (unadjusted); no multiplicity correction was applied across the four clinical outcomes in this pilot study. Welch change-score, Mann-Whitney U, permutation, and bootstrap analyses were used as sensitivity analyses.

MRI Acquisition

MRI data were acquired before and after treatment at Huashan Hospital, Hongqiao Campus, Shanghai, China, using a 3.0-T uMR 790 scanner (United Imaging Healthcare, UIH). A T1-weighted 3D inversion-recovery gradient-echo sequence was acquired in the sagittal plane (TR/TE/TI, 8.3/2.8/1080 ms; flip angle, 8 degrees; field of view, 240 x 256 mm; matrix, 320 x 300; 212 contiguous 0.8-mm slices; 0.8-mm isotropic voxels; acquisition time, 6 min 46). A complementary sagittal T2-weighted 3D fast spin-echo sequence was acquired for lesion localization during manual delineation (TR/TE, 3000/474.6 ms; flip angle, 58 degrees; echo train length, 220; field of view, 240 x 256 mm; matrix, 320 x 300; 208 contiguous 0.8-mm slices; 0.8-mm isotropic voxels; acquisition time, 4 min 33). Resting-state fMRI was acquired using a multiband factor-7 gradient-echo echo-planar imaging sequence (TR/TE, 700/30 ms; flip angle, 52 degrees; 63 axial slices; field of view, 210 x 210 mm; acquisition matrix, 84 x 84; 2.5-mm isotropic voxels with no interslice gap; 700 volumes; acquisition time, 8 min 10). Participants were instructed to remain still, keep their eyes closed, stay awake and avoid structured mental tasks.

rs-fMRI Preprocessing

Preprocessing was performed with CONN toolbox v22.a and SPM12 [28–30]. After import into CONN, images from participants with left-hemisphere lesions were left-right flipped to display the lesioned hemisphere consistently on the right before subsequent preprocessing and group-level analyses [31]. Functional series were realigned to correct head motion, temporally aligned across slices, screened for outlier scans and transformed to MNI space through an indirect normalization procedure based on the structural image [28, 29, 32, 33]. Anatomical images were segmented into gray matter, white matter and cerebrospinal-fluid compartments during normalization. Functional images were resampled to 2-mm isotropic MNI space and smoothed with a 6-mm full-width-at-half-maximum Gaussian kernel.

Artifact handling combined scan-level scrubbing and nuisance regression, with additional attention to lesion, movement and physiological confounding that can affect post-stroke fMRI analyses [32–34]. Outlier volumes were identified with ART-based criteria using framewise displacement greater than 0.9 mm and global BOLD signal change greater than 5 standard deviations. Run-level quality control was quantified from the SPM realignment parameters as mean framewise displacement (Power definition; rotations converted using a 50-mm radius), maximum frame-to-frame translational displacement, and the number of ART-flagged volumes. These indices were summarized by group and time point for retained scans (Supplementary Table S5). Four participants were excluded after imaging quality control: one REX participant because maximum head displacement exceeded 3 mm; and three control participants because one did not complete the post-intervention scan after hospital discharge and two had head motion exceeding 3 mm. The final imaging sample therefore comprised 20 participants (REX n = 11; control n = 9). Denoising included anatomical CompCor components from white matter and cerebrospinal fluid, motion parameters and their temporal derivatives, identified outlier scans, session effects and low-order temporal trends [28, 34, 35]. The residual BOLD time series were band-pass filtered at 0.008–0.09 Hz before first-level metric estimation.

First-Level Imaging Metrics

ALFF was calculated from the denoised band-pass filtered BOLD signal to quantify regional low-frequency fluctuation amplitude [36–38]. For seed-based functional connectivity, we used the side-standardized affected-side precentral gyrus parcel (PreCG_r) from the CONN default atlas, which is derived from the FSL Harvard-Oxford cortical atlas; this atlas parcel was not a coordinate-defined sphere [39, 40]. IHC maps quantified Fisher-transformed correlations between each voxel and its contralateral homotopic counterpart [41]. Bilaterally mirrored IHC peaks were treated as mirrored components of a single homotopic effect, and bilateral cluster values were averaged for subject-level summaries. LCOR maps summarized short-range local connectivity coherence within a Gaussian neighborhood, and GCOR maps summarized each voxel's average connectivity with the rest of the brain [42, 43]. LCOR and GCOR were included as exploratory supplementary measures and were not part of the main group-by-time result family.

Second-Level Imaging Statistics

Voxel wise second-level analyses were performed separately for ALFF, seed-based FC, IHC, LCOR, and GCOR using a general linear model including group (REX vs control), time (post vs pre), and the group-by-time interaction in CONN/SPM [28–30]. The group-by-time interaction was the principal contrast for assessing whether longitudinal changes differed between the two groups. Exploratory within-group pre-post contrasts were additionally examined to describe the direction of change and were not interpreted as evidence of a treatment-specific effect.

For each metric and contrast, statistical maps were thresholded at a voxel wise $P < 0.001$ uncorrected, followed by cluster-level false-discovery-rate correction at $P < 0.05$ using Gaussian random-field cluster inference. Correction was applied separately within each metric-by-contrast map; no additional correction was performed across imaging metrics or contrasts. Accordingly, results from the different imaging measures were interpreted separately rather than as a single multiplicity-adjusted imaging effect.

Brain-Behavior Analyses

For any clusters surviving the predefined threshold in the group-by-time analyses, mean imaging values were extracted for each participant, and pre-to-post changes were calculated. Associations between imaging changes and changes in clinical outcomes were examined across all participants retained for imaging analysis using Spearman rank correlations because of the small sample size and potential non-normality. These analyses were post hoc and exploratory. Correlation P values were two-sided and nominal, with no adjustment for multiple testing.

Results

Participant Flow and Baseline Characteristics

Twenty-four participants were randomized and included in the clinical analysis (REX n = 12; control n = 12), and all completed the allocated intervention and clinical follow-up. No adverse events occurred during the intervention period. After rs-fMRI quality control, 20 participants were included in imaging analyses (REX n = 11; control n = 9); the four exclusions comprised one REX participant with head motion exceeding 3 mm, one control participant who did not complete the post-intervention scan after hospital discharge, and two control participants with head motion exceeding 3 mm. Run-level motion quality control in the retained sample is reported in Supplementary Table S5. Mean framewise displacement ranged from 0.158 ± 0.038 to 0.205 ± 0.082 mm across the four group/time combinations, mean maximum frame-to-frame translation ranged from 0.283 ± 0.080 to 0.392 ± 0.154 mm, and mean ART censoring ranged from 0.87% to 3.45%. A descriptive retained-versus-excluded comparison is provided in Supplementary Table S6. Baseline characteristics and clinical scores were comparable between groups (Table 1).

Table 1
Baseline characteristics and clinical scores.

Characteristic	REX group (n = 12)	Control group (n = 12)	P value
Age, years	55.25 ± 16.18	59.08 ± 9.72	0.489
Male/female, n	7/5	5/7	0.414
Stroke type, ischemic/hemorrhagic, n	6/6	4/8	0.408
Paretic side, left/right, n	7/5	7/5	1.000
Disease duration, days	62.17 ± 51.02	82.58 ± 33.37	0.184
MoCA	24.83 ± 3.64	24.58 ± 3.92	0.873
BBS at baseline	20.67 ± 18.09	18.92 ± 15.23	0.930
FMA-LE at baseline	18.83 ± 7.41	18.42 ± 7.17	0.890
PASS at baseline	18.58 ± 10.20	16.83 ± 10.24	0.680
FAC at baseline	0.50 [0.00, 4.00]	0.50 [0.00, 3.50]	0.660

Data are mean ± SD, median [interquartile range], or n. P values are descriptive baseline comparisons.

Clinical Outcomes

After 4 weeks, baseline-adjusted BBS and FMA-LE outcomes favored REX. FAC was favorable but exploratory, whereas PASS did not show a statistically definitive between-group difference. In baseline-adjusted ANCOVA, REX was associated with higher post-intervention BBS scores than control (adjusted difference, 12.75; 95% CI, 1.45 to 24.04; P = 0.029) and higher FMA-LE scores (adjusted difference, 7.19; 95% CI, 3.71 to 10.67; P < 0.001). FAC was directionally favorable for REX in exploratory linear ANCOVA (adjusted difference, 1.26; 95% CI, 0.20 to 2.31; P = 0.022), whereas PASS did not show a statistically definitive between-group difference (adjusted difference, 3.96; 95% CI, -1.79 to 9.70; P = 0.167). ANCOVA diagnostics are reported in Supplementary Table S7. Shapiro-Wilk tests did not suggest substantial deviations from residual normality, and group-by-baseline interactions did not indicate violations of homogeneity of regression slopes; Breusch-Pagan tests indicated heteroscedasticity for BBS and PASS. HC3-robust sensitivity analyses yielded the same substantive interpretation (BBS P = 0.043; FMA-LE P = 0.001; PASS P = 0.202; FAC P = 0.031). Because FAC is ordinal, its linear ANCOVA is exploratory; the baseline-adjusted cumulative-logit sensitivity analysis was directionally consistent (REX versus control odds ratio, 8.77; 95% CI, 1.56 to 49.42; P = 0.014; Supplementary Table S8). In the rs-fMRI-retained subset, the baseline-adjusted pattern was compatible with the full-sample result: REX was associated with higher post-intervention BBS scores (adjusted difference, 13.48; 95% CI, 0.35 to 26.61; P = 0.045) and FMA-LE scores (adjusted difference, 7.15; 95% CI, 3.45 to 10.85; P < 0.001), whereas PASS and FAC remained favorable but statistically non-definitive exploratory findings (Supplementary Table S1). Change scores are shown in Table 2 and Fig. 2 to illustrate the magnitude and distribution of individual improvement.

Table 2
Baseline-adjusted clinical outcomes after 4 weeks.

Outcome	REX baseline	REX post	REX change	Control baseline	Control post	Control change	Adjusted post-intervention difference (95% CI)	ANCOVA P
BBS	20.67 ± 18.09	42.50 ± 15.96	21.83 ± 18.32	18.92 ± 15.23	28.75 ± 16.29	9.83 ± 10.17	12.75 (1.45 to 24.04)	0.029
FMA-LE	18.83 ± 7.41	30.17 ± 3.71	11.33 ± 7.22	18.42 ± 7.17	22.83 ± 5.57	4.42 ± 5.02	7.19 (3.71 to 10.67)	< 0.001
PASS	18.58 ± 10.20	29.75 ± 8.41	11.17 ± 9.40	16.83 ± 10.24	24.83 ± 8.87	8.00 ± 6.41	3.96 (-1.79 to 9.70)	0.167
FAC	1.83 ± 2.12	4.17 ± 1.40	2.33 ± 1.83	1.33 ± 1.72	2.75 ± 1.54	1.42 ± 1.16	1.26 (0.20 to 2.31)	0.022

Change = post-intervention minus baseline. Adjusted differences and P values are from ANCOVA with the corresponding baseline score as covariate. P values are two-sided and nominal.

Group-by-Time Imaging Findings

Formal group-by-time findings are summarized in Table 3 and displayed in Fig. 3. ALFF showed greater longitudinal change in the REX group than in the control group in the affected-side precuneus, non-lesioned-side lateral occipital cortex and non-lesioned-side inferior frontal gyrus; each showed an increase in the REX group and a decrease in the control group. PreCG_r seed-based FC showed a group-by-time interaction with the affected-side middle temporal gyrus, indicating greater REX-related connectivity change than control. IHC showed bilaterally mirrored precuneus/PCC peaks representing one homotopic interhemispheric effect, with greater REX-related IHC increase than control. LCOR and GCOR had no significant group-by-time interaction and are reported only as exploratory within-group results.

Table 3
Group-by-time rs-fMRI findings.

Measure	Peak region	Peak MNI	Cluster extent, k	Cluster P-FDR	Direction
ALFF	Affected-side precuneus	+ 4, -64, + 26	31	0.013989	REX increase; control decrease
ALFF	Non-lesioned-side lateral occipital cortex	-46, -70, + 18	26	0.017534	REX increase; control decrease
ALFF	Non-lesioned-side inferior frontal gyrus	-40, + 34, +16	24	0.017534	REX increase; control decrease
PreCG_r seed-based FC	Affected-side middle temporal gyrus	+ 64, -8, -28	117	0.000206	Greater REX-related FC change than control
IHC	Bilateral precuneus/PCC homotopic effect	± 6, -54, + 22	42 per cluster	0.000101	Greater REX-related IHC increase than control

Corresponds to Fig. 3. *Images were side-standardized before analysis: negative x/left display denotes the non-lesioned side and positive x/right display denotes the affected side. Coordinates are in side-standardized MNI space. Voxel-level P < 0.001, uncorrected; cluster-level P-FDR < 0.05. Left, non-lesioned side; Right, affected side.*

Exploratory Brain-Behavior Associations

Exploratory pooled brain-behavior correlations across all imaging-retained participants are shown in Fig. 5; the complete matrix is given in Supplementary Table S4. Affected-side precuneus Delta ALFF was associated with Delta BBS (rho = 0.577, P = 0.008) and Delta FMA-LE (rho = 0.501, P = 0.024), and non-lesioned-side inferior frontal Delta ALFF was associated with Delta BBS (rho = 0.490, P = 0.028). For the formal PreCG_r-to-affected-side MTG FC cluster, associations were observed with Delta BBS (rho = 0.447, P = 0.048) and Delta FMA-LE (rho = 0.559, P = 0.010). These pooled results are exploratory observations and do not establish group-specific clinical-neural mechanisms, mediation, or causality.

Exploratory Within-Group rs-fMRI Findings

Within-group maps are summarized in Supplementary Table S3 and Fig. 4 and are interpreted only as supportive directionality information. In the REX group, exploratory pre-to-post changes included increased PreCG_r seed-based FC with the affected-side middle temporal gyrus and decreased FC with the non-lesioned cerebellum/vermis IV/V. Additional within-group changes were observed in homotopic middle frontal IHC and exploratory local/global correlation measures involving posterior association regions. These findings did not show significant group-by-time interactions and are therefore interpreted as exploratory within-group observations rather than treatment-specific effects. They do not independently demonstrate a specific visuomotor or cortico-cerebellar recovery loop.

Exploratory LCOR and GCOR Findings

LCOR and GCOR group-by-time interactions did not reach significance. In the REX group, exploratory within-group increases were observed in local correlation at the non-lesioned lateral occipital/posterior middle temporal region and affected-side precuneus/PCC, and in global correlation at the non-lesioned superior lateral occipital/angular region. In the control group, exploratory decreases were observed at affected-side superior lateral occipital peaks. These maps are shown in Fig. 4 and Supplementary Table S3 for descriptive completeness only.

Discussion

In this pilot randomized neuroimaging study, baseline-adjusted clinical results favored REX for BBS and FMA-LE. FAC was also favorable, but was exploratory; PASS did not show a clear between-group difference. In the imaging-retained sample, ALFF, PreCG_r seed-based FC and IHC showed formal group-by-time effects. LCOR and GCOR did not show group-by-time interactions, and the cerebellum/vermis result was observed only in the REX pre-post comparison.

The clinical findings should be interpreted in relation to studies using comparable devices and control conditions. The earlier independent REX trial also found favorable balance-related effects after 4 weeks [3]. More broadly, electromechanical gait training may improve the likelihood of independent walking, but reported effects differ by recovery stage and trial design [6]. Results from overground exoskeleton trials are also mixed, particularly when control participants receive active gait or upright training [44, 45]. Recent wearable-exoskeleton trials further suggest that patient selection and the content of the protocol influence the observed effect [46, 47]. In the present study, the control programme matched treatment time and therapist contact. However, it could not match the mechanical support, feedback and repeated weight-shift demands of the REX device. These differences should be considered when comparing the two interventions.

The different findings for BBS/FMA-LE and PASS should not be overlooked. Although BBS and PASS both assess balance-related performance, they contain different tasks and may not have the same responsiveness [48]. PASS is particularly useful in the early phase after stroke and can predict subsequent mobility, but a 4-week intervention may affect its items differently from the functional balance tasks emphasized in BBS [49]. Its validity across stroke stages is another reason to report the null PASS result directly [50]. Our findings therefore do not show that REX improved every component of postural control. The clearer pilot signals were seen in functional balance capacity and lower-limb motor impairment.

The affected-side precuneus showed an ALFF interaction, and IHC showed bilaterally mirrored precuneus/PCC peaks representing one homotopic effect. The precuneus has been linked to visuospatial processing, body-related representation and large-scale network organization [51]. However, it is not a unitary balance region [52]. As part of the default-mode network, it may also show resting-state changes that are not specific to posture [53]. In the context of supported upright REX training, the posterior-midline findings may be related to body-position monitoring or multisensory integration. Other explanations remain

possible, including general recovery, changes in attention during scanning, lesion-related reorganization and sampling variation. The proximity of the ALFF and IHC findings is an observation across measures; it does not show that the precuneus/PCC mediated clinical improvement.

The LOC and MTG findings may be relevant to visual-motor processing, but they should not be treated as one established pathway. Postural control requires visual and association systems when body orientation is adjusted from ongoing sensory feedback [54]. In this study, the LOC finding was an ALFF interaction, whereas the affected-side MTG finding was a PreCG_r seed-based FC interaction. These were different measures at different peaks. Association-cortex activity has been related to motor recovery in moderate-to-severe stroke [55], but its meaning depends on lesion characteristics and task context. In addition, post-stroke motor connectivity can change in directions that are not simply equivalent to better function [16]. Accordingly, the current findings provide a possible visual-association and motor-association interpretation.

The frontal and cerebellar findings also require different levels of interpretation. The inferior frontal ALFF interaction may reflect changes in executive-attentional demand, action monitoring or adjustment to postural error during difficult upright tasks [56]. The bilateral middle-frontal IHC increase was observed only in the REX within-group contrast and is not treatment-specific. The PreCG_r–MTG FC finding was supported by a formal group-by-time interaction, whereas the cerebellum/vermis FC decrease was observed only in the REX pre-to-post comparison and should be interpreted as an exploratory within-group change. Cerebellar circuits are involved in sensorimotor calibration and communicate with several cortical networks [57]. Neuroimaging studies also support a role for cerebellar and supraspinal systems in posture and gait [58, 59]. Related work also shows that cerebellar function cannot be separated from its wider cortical and basal-ganglia connections [60]. However, these studies do not define the expected direction of a training-related FC change. The reduction in cerebellar FC in the present study could reflect recalibration, reduced compensation, baseline differences or statistical variation. It cannot be taken as direct evidence of greater network efficiency or recovery.

The LCOR and GCOR findings place an important boundary on interpretation. Neither measure showed a formal group-by-time interaction, and therefore the present data do not support a broad increase in local or global connectivity after REX. However, some exploratory within-group LCOR/GCOR changes spatially overlapped with regions identified in the formal ALFF and IHC analyses, including posterior association and precuneus/PCC regions. These observations provide hypothesis-generating supportive context but should not be interpreted as independent treatment effects or confirmatory replications. The pooled brain-behavior correlations also need to be read cautiously: they combined both groups, were post hoc and used nominal P values; they do not test a REX-specific association or mediation. The small clinical sample, the 20-person imaging subset, numerical differences in disease duration and stroke type, post-stroke hemodynamic distortion, and the limits of extracted-value covariate models are all relevant [61]. Motion control reduces, but cannot remove, these concerns [32]. Head motion can affect resting-state estimates even after extensive nuisance regression [33]. The reliability of low-frequency resting-state measures is a further reason to treat this pilot as a source of effect estimates, not a biomarker-discovery study [38]. A larger preregistered trial should define multiplicity across imaging measures, include objective gait and

balance outcomes and longer follow-up, and test whether the posterior-midline and motor-association findings can be reproduced.

Conclusion

REX-assisted lower-limb rehabilitation was associated with favorable balance and lower-limb motor outcomes in this pilot trial. Cluster-corrected group-by-time associations were observed for ALFF, right precentral-gyrus seed-based FC and IHC. These findings highlighted posterior-midline, visual-association and frontal regions as candidate training-related correlates. The cerebellar finding was observed only in a REX within-group contrast, and LCOR/GCOR group-by-time interactions were not significant. Larger randomized neuroimaging studies should prespecify clinical and imaging endpoints and multiplicity plans and test whether these candidate findings are reproducible.

Abbreviations

Declarations

Ethics approval and consent to participate:

This study was performed in accordance with the Declaration of Helsinki and was approved by the Ethics Committee of Shanghai Hebin Rehabilitation Hospital (Approval No. HBRH-MEC2023004). All participants provided written informed consent before participation.

Consent for publication:

Not applicable.

Competing interests:

The authors declare that they have no competing interests.

Funding:

This work was supported by the National Natural Science Foundation of China (82102665), the Shanghai Sailing Program (21YF1404600) and the Shanghai Minhang District Medical Specialty Construction Project (2025MWFC03).

Author Contribution

Hewei Wang, Ling Ding and Yanzheng Zhang conceived and designed the study. Yuanyuan Chu, Zhe Li and Liwang Deng performed the experiments and collected the data. Hewei Wang, Qijin Zhai and Yang Wang

were responsible for data curation and statistical analysis. Zhichao Liu and Limin Sun assisted in the investigation and methodology. Yanzheng Zhang and Yang Wang drafted the original manuscript. Hewei Wang, Qijin Zhai, Yulin Li, Bin Su, Wei Sun, Yanjie Hu and Ling Ding reviewed and edited the manuscript. Hewei Wang supervised the entire project. All authors have read and approved the final manuscript.

Acknowledgement

We would like to express our gratitude to all the volunteers who participated in this study. We would like to express our sincere gratitude to Shurui Zhang, Canxin Zhou, Xinna Tan, Jingyan Cheng, Ling He, Guomin Fan, Wei Dou, Donghe Li, Shu Zhu and Weicheng Zhao for their efforts in data collation and figure drawing.

Availability of data and materials:

The datasets used and/or analyzed during the current study are available from the corresponding author on reasonable request.

References

1. MaQ,LiR,WangL,YinP,WangY,YanC,etal.Temporal trend and attributable risk factors of stroke burden in China, 1990–2019: an analysis for the Global Burden of Disease Study 2019.Lancet Public Health.2021;6:e897–906.https://doi.org/10.1016/s2468-2667(21)00228-0.
2. LanghorneP,BernhardtJ,KwakkelG.Stroke rehabilitation.Lancet Lond Engl.2011;377:1693–702.https://doi.org/10.1016/S0140-6736(11)60325-5.
3. ZhangY,ZhaoW,WanC,WuX,HuangJ,WangX,etal.Exoskeleton rehabilitation robot training for balance and lower limb function in sub-acute stroke patients: a pilot, randomized controlled trial.J NeuroEngineering Rehabil [Internet].2024;21.https://doi.org/10.1186/s12984-024-01391-0.
4. CramerSC.Repairing the human brain after stroke: I. Mechanisms of spontaneous recovery.Ann Neurol.2008;63:272–87.https://doi.org/10.1002/ana.21393.
5. WinsteinCJ,SteinJ,ArenaR,BatesB,CherneyLR,CramerSC,etal.Guidelines for Adult Stroke Rehabilitation and Recovery.Stroke [Internet].2016;47.https://doi.org/10.1161/str.0000000000000098.
6. MehrholzJ,KuglerJ,PohlM,ElsnerB.Electromechanical-assisted training for walking after stroke.Cochrane Database Syst Rev [Internet].2025;2025.https://doi.org/10.1002/14651858.cd006185.pub6.
7. LouieDR,EngJJ.Powered robotic exoskeletons in post-stroke rehabilitation of gait: a scoping review.J NeuroEngineering Rehabil [Internet].2016;13.https://doi.org/10.1186/s12984-016-0162-5.
8. WuL,XuG,WuQ.The effect of the Lokomat® robotic-orthosis system on lower extremity rehabilitation in patients with stroke: a systematic review and meta-analysis.Front Neurol [Internet].2023;14.https://doi.org/10.3389/fneur.2023.1260652.

9. HuM,WangS,WuC,LiK,GengZ,XuG,etal.Efficacy of robot-assisted gait training on lower extremity function in subacute stroke patients: a systematic review and meta-analysis.J NeuroEngineering Rehabil [Internet].2024;21.https://doi.org/10.1186/s12984-024-01463-1.
10. WangH,ShenH,HanY,ZhouW,WangJ.Effect of robot-assisted training for lower limb rehabilitation on lower limb function in stroke patients: a systematic review and meta-analysis.Front Hum Neurosci [Internet].2025;19.https://doi.org/10.3389/fnhum.2025.1549379.
11. LeeJH,KimG.Effectiveness of Robot-Assisted Gait Training in Stroke Rehabilitation: A Systematic Review and Meta-Analysis.J Clin Med.2025;14:4809.https://doi.org/10.3390/jcm14134809.
12. LeeM-H,TianM-Y,KimM-K.The Effectiveness of Overground Robot Exoskeleton Gait Training on Gait Outcomes, Balance, and Motor Function in Patients with Stroke: A Systematic Review and Meta-Analysis of Randomized Controlled Trials.Brain Sci.2024;14:834.https://doi.org/10.3390/brainsci14080834.
13. HuoC,ShaoG,ChenT,LiW,WangJ,XieH,etal.Effectiveness of unilateral lower-limb exoskeleton robot on balance and gait recovery and neuroplasticity in patients with subacute stroke: a randomized controlled trial.J NeuroEngineering Rehabil [Internet].2024;21.https://doi.org/10.1186/s12984-024-01493-9.
14. MoroneG,AnnicchiaricoR,IosaM,FedericiA,PaolucciS,CortésU,etal.Overground walking training with the i-Walker, a robotic servo-assistive device, enhances balance in patients with subacute stroke: a randomized controlled trial.J Neuroengineering Rehabil.2016;13:47.https://doi.org/10.1186/s12984-016-0155-4.
15. JayaramanA,O'BrienMK,MadhavanS,MummidisettyCK,RothHR,HohlK,etal.Stride management assist exoskeleton vs functional gait training in stroke: A randomized trial.Neurology.2019;92:e263–73.https://doi.org/10.1212/WNL.0000000000006782.
16. GrefkesC,FinkGR.Connectivity-based approaches in stroke and recovery of function.Lancet Neurol.2014;13:206–16.https://doi.org/10.1016/s1474-4422(13)70264-3.
17. CarterAR,ShulmanGL,CorbettaM.Why use a connectivity-based approach to study stroke and recovery of function? NeuroImage.2012;62:2271–80.https://doi.org/10.1016/j.neuroimage.2012.02.070.
18. ParkC,ChangWH,OhnSH,KimST,BangOY,Pascual-LeoneA,etal.Longitudinal changes of resting-state functional connectivity during motor recovery after stroke.Stroke.2011;42:1357–62.https://doi.org/10.1161/STROKEAHA.110.596155.
19. TangZ,ZhaoY,SunX,LiuY,SuW,LiuT,etal.Evidence that robot-assisted gait training modulates neuroplasticity after stroke: An fMRI pilot study based on graph theory analysis.Brain Res.2024;1842:149113.https://doi.org/10.1016/j.brainres.2024.149113.
20. NijboerTCW,BumaFE,WintersC,VansteenselMJ,KwakkelG,RamseyNF,etal.No changes in functional connectivity during motor recovery beyond 5 weeks after stroke; A longitudinal resting-state fMRI study.PLOS ONE.2017;12:e0178017.https://doi.org/10.1371/journal.pone.0178017.
21. KraeutnerSN,RubinoC,RinatS,LakhaniB,BorichMR,WaddenKP,etal.Resting State Connectivity Is Modulated by Motor Learning in Individuals After Stroke.Neurorehabil Neural Repair.2021;35:513–24.https://doi.org/10.1177/15459683211006713.

22. YuH,WangH,LiuS,JingJ,HuangG,ZhangY,etal.Post-task resting-state fMRI of walking-related neural activity in patients with stroke: immediate and delayed brain network dynamics.Ann Med [Internet].2026;58.https://doi.org/10.1080/07853890.2026.2662817.
23. CharalambousCC,BowdenMG,AdkinsDL.Motor Cortex and Motor Cortical Interhemispheric Communication in Walking After Stroke.Neurorehabil Neural Repair.2016;30:94–102.https://doi.org/10.1177/1545968315581418.
24. GladstoneDJ,DanellsCJ,BlackSE.The Fugl-Meyer Assessment of Motor Recovery after Stroke: A Critical Review of Its Measurement Properties.Neurorehabil Neural Repair.2002;16:232–40.https://doi.org/10.1177/154596802401105171.
25. KwongPWH,NgSSM.Cutoff Score of the Lower-Extremity Motor Subscale of Fugl-Meyer Assessment in Chronic Stroke Survivors: A Cross-Sectional Study.Arch Phys Med Rehabil.2019;100:1782–7.https://doi.org/10.1016/j.apmr.2019.01.027.
26. HoldenMK,GillKM,MagliozziMR,NathanJ,Piehl-BakerL.Clinical gait assessment in the neurologically impaired. Reliability and meaningfulness.Phys Ther.1984;64:35–40.https://doi.org/10.1093/ptj/64.1.35.
27. EldridgeSM,ChanCL,CampbellMJ,BondCM,HopewellS,ThabaneL,etal.CONSORT 2010 statement: extension to randomised pilot and feasibility trials.BMJ.2016;355:i5239.https://doi.org/10.1136/bmj.i5239.
28. Whitfield-GabrieliS,Nieto-CastanonA.Conn: a functional connectivity toolbox for correlated and anticorrelated brain networks.Brain Connect.2012;2:125–41.https://doi.org/10.1089/brain.2012.0073.
29. PennyWD,FristonKJ,AshburnerJT,KiebelSJ,NicholsTE.Statistical parametric mapping: the analysis of functional brain images.Elsevier;2011.
30. Nieto-CastanonA.Handbook of functional connectivity magnetic resonance imaging methods in CONN.Hilbert Press;2020.
31. WangH,XiongX,ZhangK,WangX,SunC,ZhuB,etal.Motor network reorganization after motor imagery training in stroke patients with moderate to severe upper limb impairment.CNS Neurosci Ther.2023;29:619–32.https://doi.org/10.1111/cns.14065.
32. PowerJD,BarnesKA,SnyderAZ,SchlaggarBL,PetersenSE.Spurious but systematic correlations in functional connectivity MRI networks arise from subject motion.NeuroImage.2012;59:2142–54.https://doi.org/10.1016/j.neuroimage.2011.10.018.
33. SatterthwaiteTD,WolfDH,LougheadJ,RuparelK,ElliottMA,HakonarsonH,etal.Impact of in-scanner head motion on multiple measures of functional connectivity: Relevance for studies of neurodevelopment in youth.NeuroImage.2012;60:623–32.https://doi.org/10.1016/j.neuroimage.2011.12.063.
34. BrihmatN,BoulanouarK,DarmanaR.Controlling for lesions, kinematics and physiological noise: impact on fMRI results of spastic post-stroke patients.MethodsX.2020;7:101056.https://doi.org/10.1016/j.mex.2020.101056.
35. BehzadiY,RestomK,LiauJ,LiuT.A component based noise correction method (CompCor) for BOLD and perfusion based fMRI.NeuroImage.2007;37:90–101.https://doi.org/10.1016/j.neuroimage.2007.04.042.

36. ZangY,HeY,ZhuC.Altered baseline brain activity in children with ADHD revealed by resting-state functional MRI.Brain Dev.2007;29:83–91.https://doi.org/10.1016/j.braindev.2006.07.002.
37. YangH,LongX,YangY.Amplitude of low frequency fluctuation within visual areas revealed by resting-state functional MRI.NeuroImage.2007;36:144–52.https://doi.org/10.1016/j.neuroimage.2007.01.054.
38. ZuoX-N,DiMartinoA,KellyC,ShehzadZE,GeeDG,KleinDF,etal.The oscillating brain: Complex and reliable.NeuroImage.2010;49:1432–45.https://doi.org/10.1016/j.neuroimage.2009.09.037.
39. HampsonM,PetersonB,SkudlarskiP,GatenbyJ,GoreJ.Detection of functional connectivity using temporal correlations in MR images.Hum Brain Mapp.2002;15:247–62.https://doi.org/10.1002/hbm.10022.
40. BiswalB,YetkinF,HaughtonV,HydeJ.Functional connectivity in the motor cortex of resting human brain using echo-planar MRI.Magn Reson Med.1995;34:537–41.https://doi.org/10.1002/mrm.1910340409.
41. JinX,LiangX,GongG.Functional Integration Between the Two Brain Hemispheres: Evidence From the Homotopic Functional Connectivity Under Resting State.Front Neurosci [Internet].2020;https://doi.org/10.3389/fnins.2020.00932.
42. DeshpandeG,LaConteS,PeltierS,HuX.Integrated local correlation: a new measure of local coherence in fMRI data.Hum Brain Mapp.2009;30:13–23.https://doi.org/10.1002/hbm.20482.
43. SaadZ,ReynoldsR,JoH.Correcting brain-wide correlation differences in resting-state FMRI.Brain Connect.2013;3:339–52.https://doi.org/10.1089/brain.2013.0156.
44. YangJ,GongY,YuL,PengL,CuiY,HuangH.Effect of exoskeleton robot-assisted training on gait function in chronic stroke survivors: a systematic review of randomised controlled trials.BMJ Open.2023;13:e074481.https://doi.org/10.1136/bmjopen-2023-074481.
45. JinY,XiongB,ChenL,ZhaoW,LiZ,ZhangC,etal.Efficacy and safety of using a unilateral lower limb exoskeleton combined with conventional treatment in post-stroke rehabilitation: a randomized controlled trial.Front Bioeng Biotechnol [Internet].2024;12.https://doi.org/10.3389/fbioe.2024.1441986.
46. ChangWH,KimT-W,KimHS,HanapiahFA,LeeJW,HanS-H,etal.Efficacy of Wearable Exoskeleton for Gait Recovery in Patients With Stroke: A Multicenter Randomized Controlled Trial.Stroke.2026;57:577–86.https://doi.org/10.1161/strokeaha.125.052763.
47. HanYK,KimKH,SonJE,JeonA,LeeHB,LeeM,etal.Effects of Robot-Assisted Gait Training on Stage-Based Lower Limb Motor Recovery and Muscle Tone in Subacute Stroke: A Randomized Controlled Trial.J Clin Med [Internet].2026;15.https://doi.org/10.3390/jcm15072514.
48. BenaimC,PérennouDA,VillyJ,RousseauxM,PelissierJY.Validation of a Standardized Assessment of Postural Control in Stroke Patients.Stroke.1999;30:1862–8.https://doi.org/10.1161/01.str.30.9.1862.
49. HuangY,WangW,LiouT,LiaoC,LinL,HuangS.Postural Assessment Scale for Stroke Patients Scores as a predictor of stroke patient ambulation at discharge from the rehabilitation ward.J Rehabil Med.2016;48:259–64.https://doi.org/10.2340/16501977-2046.
50. Estrada-BarrancoC,Cano-de-la-CuerdaR,Abuín-PorrasV,Molina-RuedaF.Postural Assessment Scale for Stroke Patients in Acute, Subacute and Chronic Stage: A Construct Validity

Study.Diagnostics.2021;11:365.https://doi.org/10.3390/diagnostics11020365.

51. CavannaAE,TrimbleMR.The precuneus: a review of its functional anatomy and behavioural correlates.Brain.2006;129:564–83.https://doi.org/10.1093/brain/awl004.
52. DadarioNB,SughrueME.The functional role of the precuneus.Brain J Neurol.2023;146:3598–607.https://doi.org/10.1093/brain/awad181.
53. UtevskyAV,SmithDV,HuettelSA.Precuneus is a functional core of the default-mode network.J Neurosci Off J Soc Neurosci.2014;34:932–40.https://doi.org/10.1523/JNEUROSCI.4227-13.2014.
54. DijkstraBW,BekkersEMJ,GilatM,deRondV,HardwickRM,NieuwboerA.Functional neuroimaging of human postural control: A systematic review with meta-analysis.Neurosci Biobehav Rev.2020;115:351–62.https://doi.org/10.1016/j.neubiorev.2020.04.028.
55. HannanuFF,ZeffiroTA,LamalleL,HeckO,RenardF,ThuriotA,etal.Parietal operculum and motor cortex activities predict motor recovery in moderate to severe stroke.NeuroImage Clin.2017;14:518–29.https://doi.org/10.1016/j.nicl.2017.01.023.
56. TakakusakiK.Functional Neuroanatomy for Posture and Gait Control.J Mov Disord.2017;10:1–17.https://doi.org/10.14802/jmd.16062.
57. BucknerRL,KrienenFM,CastellanosA,DiazJC,YeoBTT.The organization of the human cerebellum estimated by intrinsic functional connectivity.J Neurophysiol.2011;106:2322–45.https://doi.org/10.1152/jn.00339.2011.
58. STOODLEYC,SCHMAHMANNJ.Functional topography in the human cerebellum: A meta-analysis of neuroimaging studies.NeuroImage.2009;44:489–501.https://doi.org/10.1016/j.neuroimage.2008.08.039.
59. JahnK,DeutschländerA,StephanT,KallaR,WiesmannM,StruppM,etal.Imaging human supraspinal locomotor centers in brainstem and cerebellum.NeuroImage.2008;39:786–92.https://doi.org/10.1016/j.neuroimage.2007.09.047.
60. BostanAC,StrickPL.The Cerebellum and Basal Ganglia are Interconnected.Neuropsychol Rev.2010;20:261–70.https://doi.org/10.1007/s11065-010-9143-9.
61. SiegelJS,SnyderAZ,RamseyL,ShulmanGL,CorbettaM.The effects of hemodynamic lag on functional connectivity and behavior after stroke.J Cereb Blood Flow Metab.2016;36:2162–76.https://doi.org/10.1177/0271678x15614846.

Figures

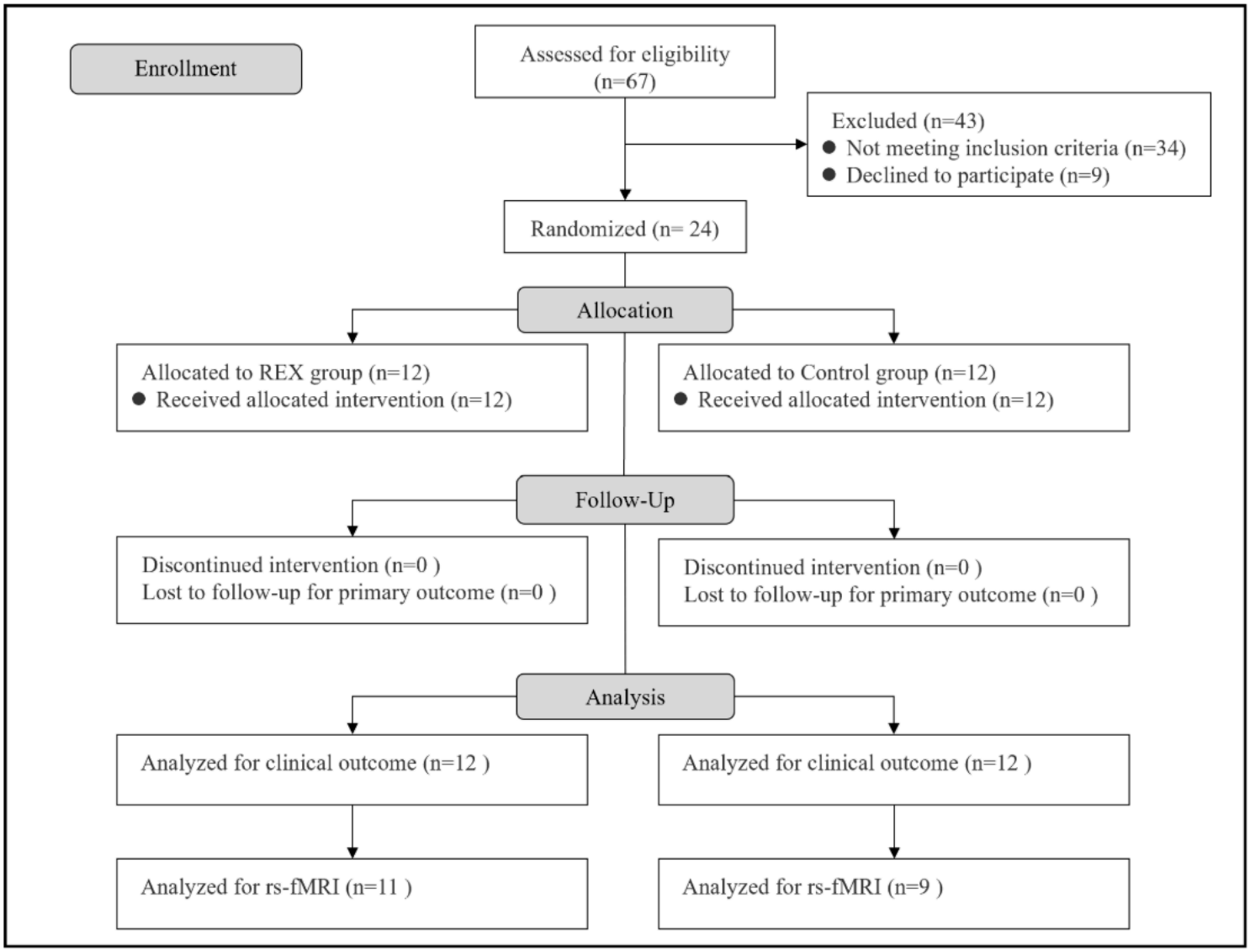


Figure 1

CONSORT-style participant flow for the pilot randomized neuroimaging study. Twenty-four patients were randomized and included in the clinical analysis. After rs-fMRI quality control procedures, 20 participants were retained for neuroimaging analyses (REX, n=11; control, n=9).

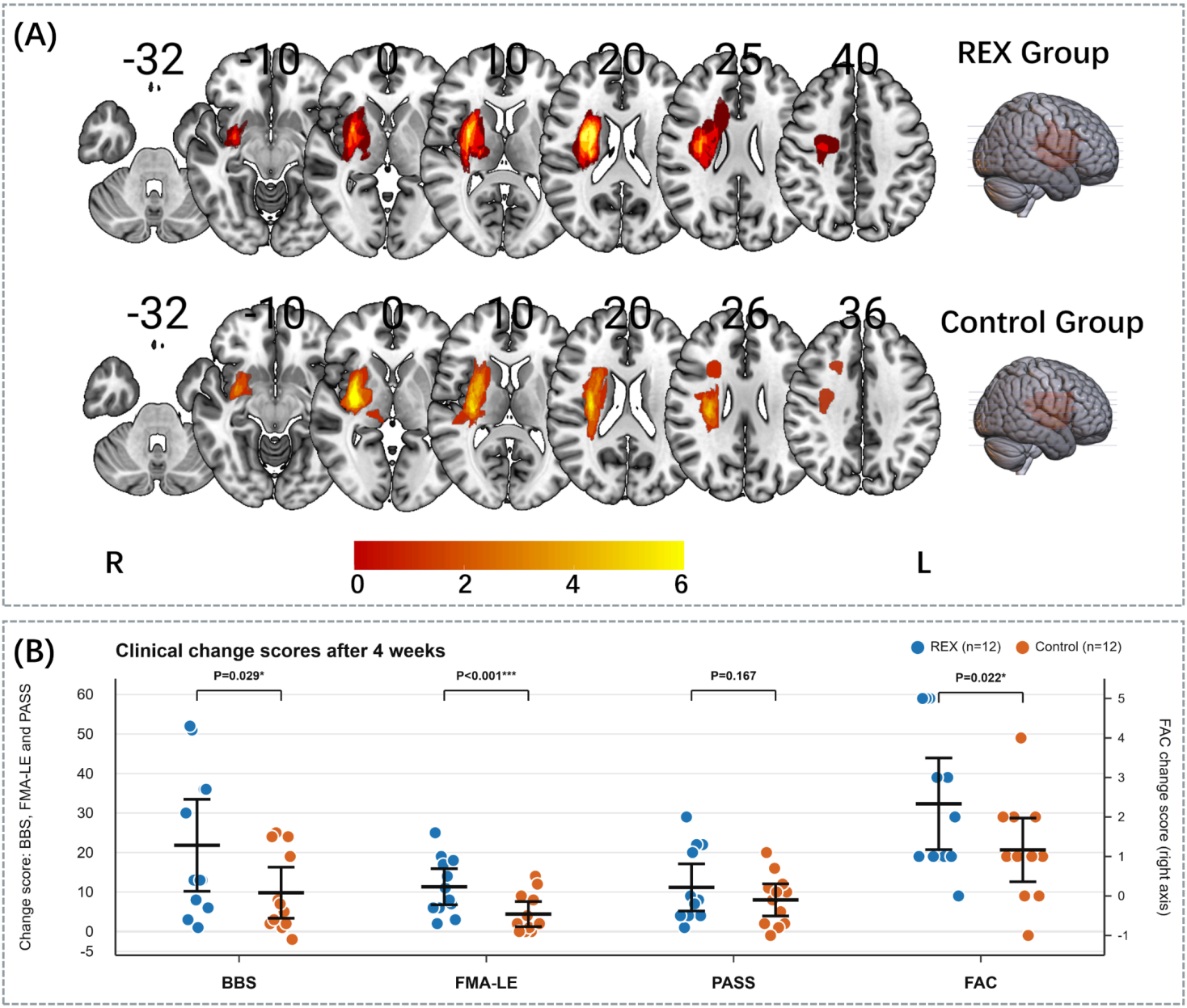


Figure 2

Lesion distribution and clinical change outcomes. (A) Lesion overlap map and lesion-volume comparison in the 20 participants retained for neuroimaging analyses (REX, n=11; control, n=9). Individual lesion masks were normalized to Montreal Neurological Institute space and side-standardized by left-right flipping when required; thus, the left and right sides of the display represent the non-lesioned and affected sides, respectively. Warmer colours indicate a greater number of participants with lesion involvement at each voxel. Lesions were predominantly located in deep subcortical structures and adjacent white matter. Lesion volume did not differ significantly between groups (REX, 6.39 ± 4.41 mL; control, 7.56 ± 2.46 mL; P=0.464). (B) Clinical change scores after 4 weeks in the full randomized sample (REX, n=12; control, n=12). Dots represent individual changes from baseline; horizontal bars indicate group means and vertical bars indicate approximate 95% confidence intervals. P values are nominal, two-sided baseline-adjusted ANCOVA results for the treatment-group effect on post-intervention scores. BBS, FMA-LE, and PASS use

the left y-axis; FAC uses the right y-axis. Positive values indicate improvement. BBS, Berg Balance Scale; FMA-LE, Fugl-Meyer Assessment Lower Extremity; PASS, Postural Assessment Scale for Stroke; FAC, Functional Ambulation Category.

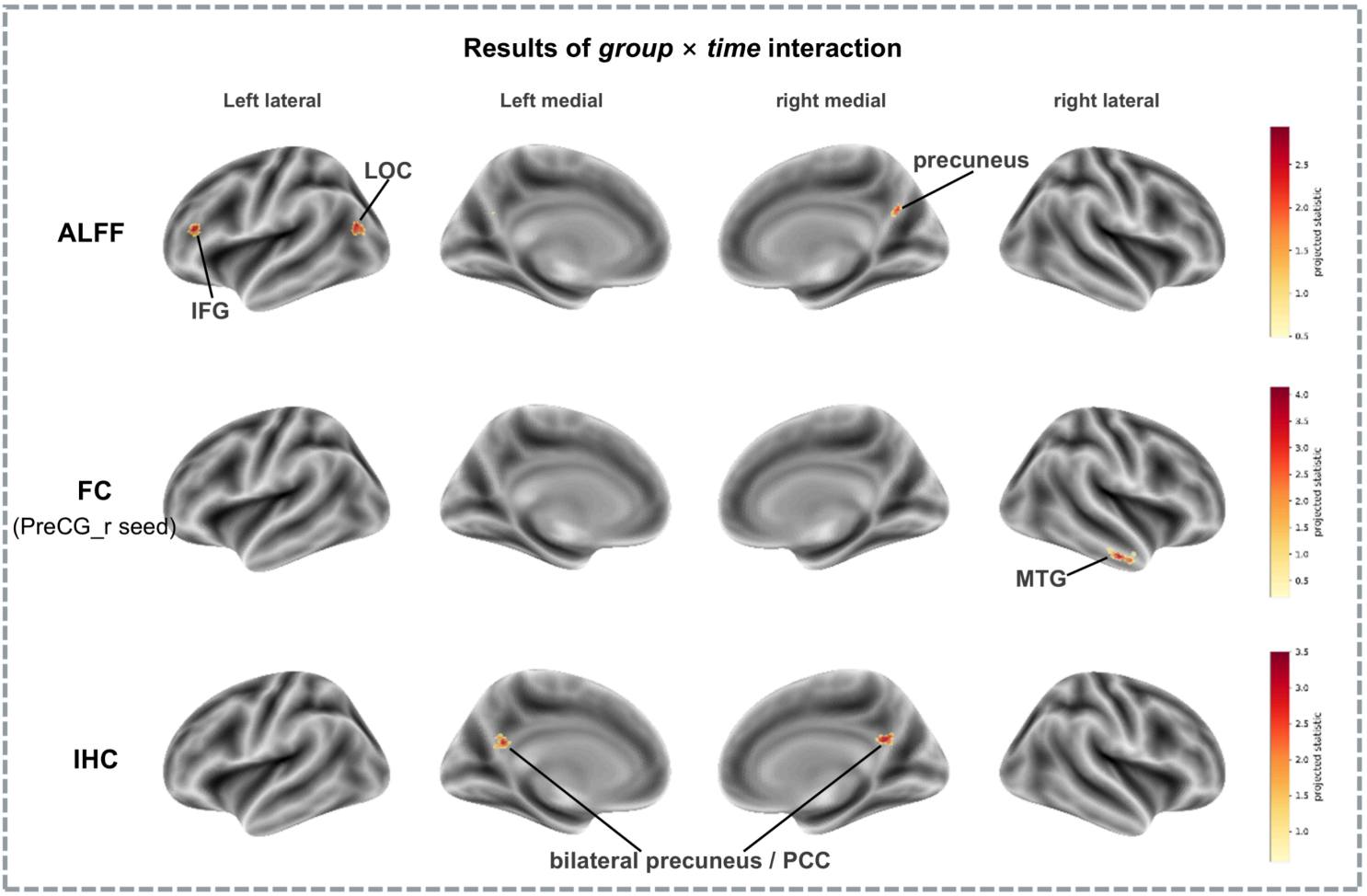


Figure 3

Group-by-time rs-fMRI findings. Thresholded group-by-time interaction maps for amplitude of low-frequency fluctuations (ALFF), seed-based functional connectivity (FC), and interhemispheric correlation (IHC) in the imaging-retained sample. ALFF interaction clusters were located in the left inferior frontal gyrus, left lateral occipital cortex, and right precuneus. Right precentral-gyrus parcel (PreCG_r) seed-based FC showed a group-by-time interaction with the right middle temporal gyrus. IHC showed a bilateral mirrored precuneus effect, representing one homotopic interhemispheric finding. Labels identify cluster peak regions; cluster extensions are reported in the results table. Maps are projected to inflated cortical surfaces. Threshold: voxel-level $P < 0.001$ uncorrected and cluster-level P-FDR < 0.05. Left, non-lesioned side; Right, affected side.

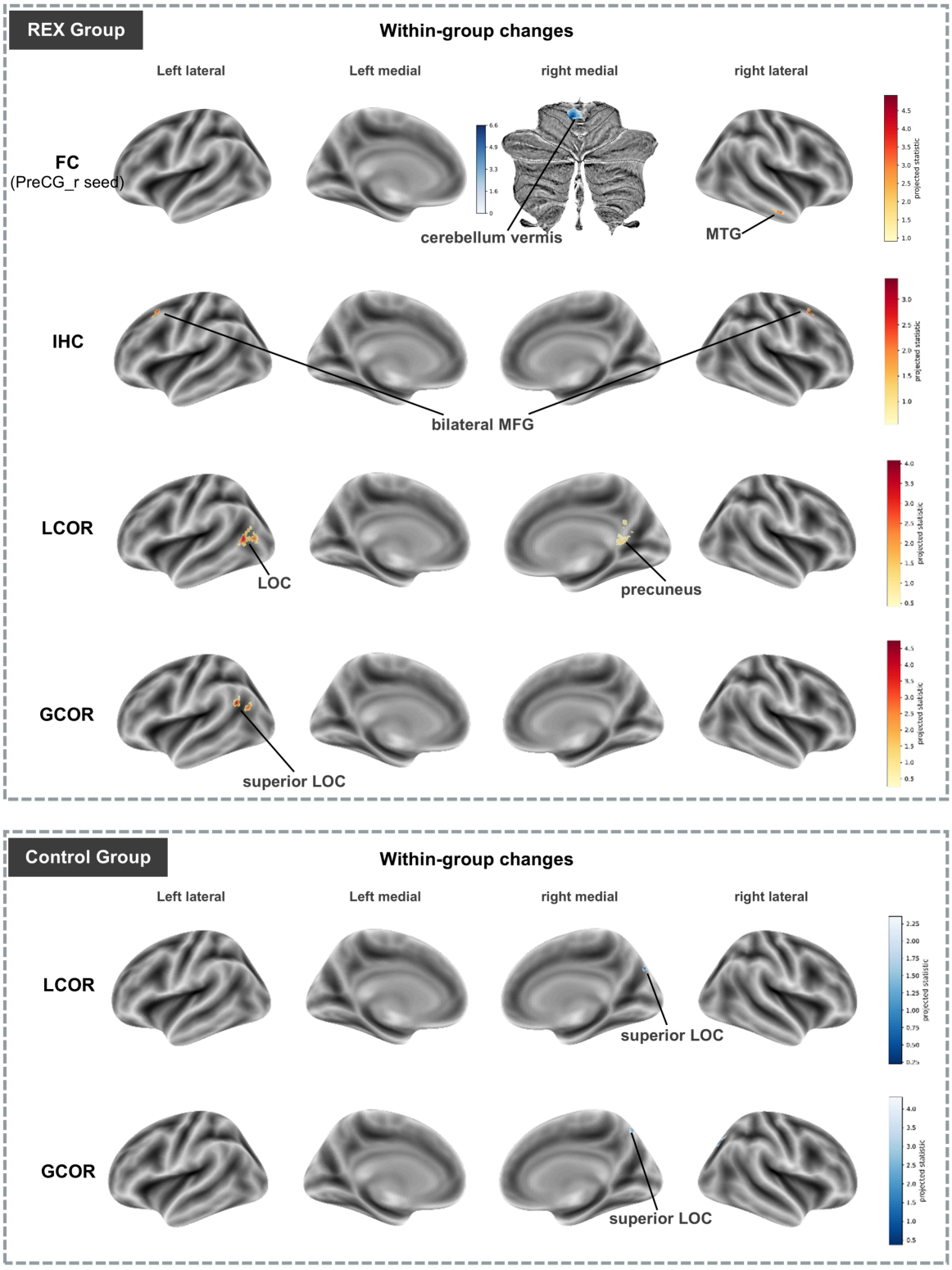


Figure 4

Exploratory within-group rs-fMRI changes. Within-group pre-to-post rs-fMRI changes in the REX and control groups. In the REX group, warm-coloured maps indicate post-intervention increases in PreCG_r seed-based FC with the right middle temporal gyrus, bilateral middle frontal gyrus IHC, local correlation in the left lateral occipital cortex and right precuneus, and global correlation in the left superior lateral occipital cortex. The blue cerebellar map indicates a post-intervention decrease in PreCG_r seed-based FC at the

cerebellum/vermis IV/V peak within the REX group. In the control group, blue maps indicate post-intervention decreases in local and global correlation at right superior lateral occipital cortical peaks. Labels identify cluster peak regions only. These within-group maps are supportive and hypothesis-generating, and do not replace the formal group-by-time tests; LCOR and GCOR showed no significant group-by-time interaction. Threshold: voxel-level P < 0.001 uncorrected and cluster-level P-FDR < 0.05. Left, non-lesioned side; Right, affected side.

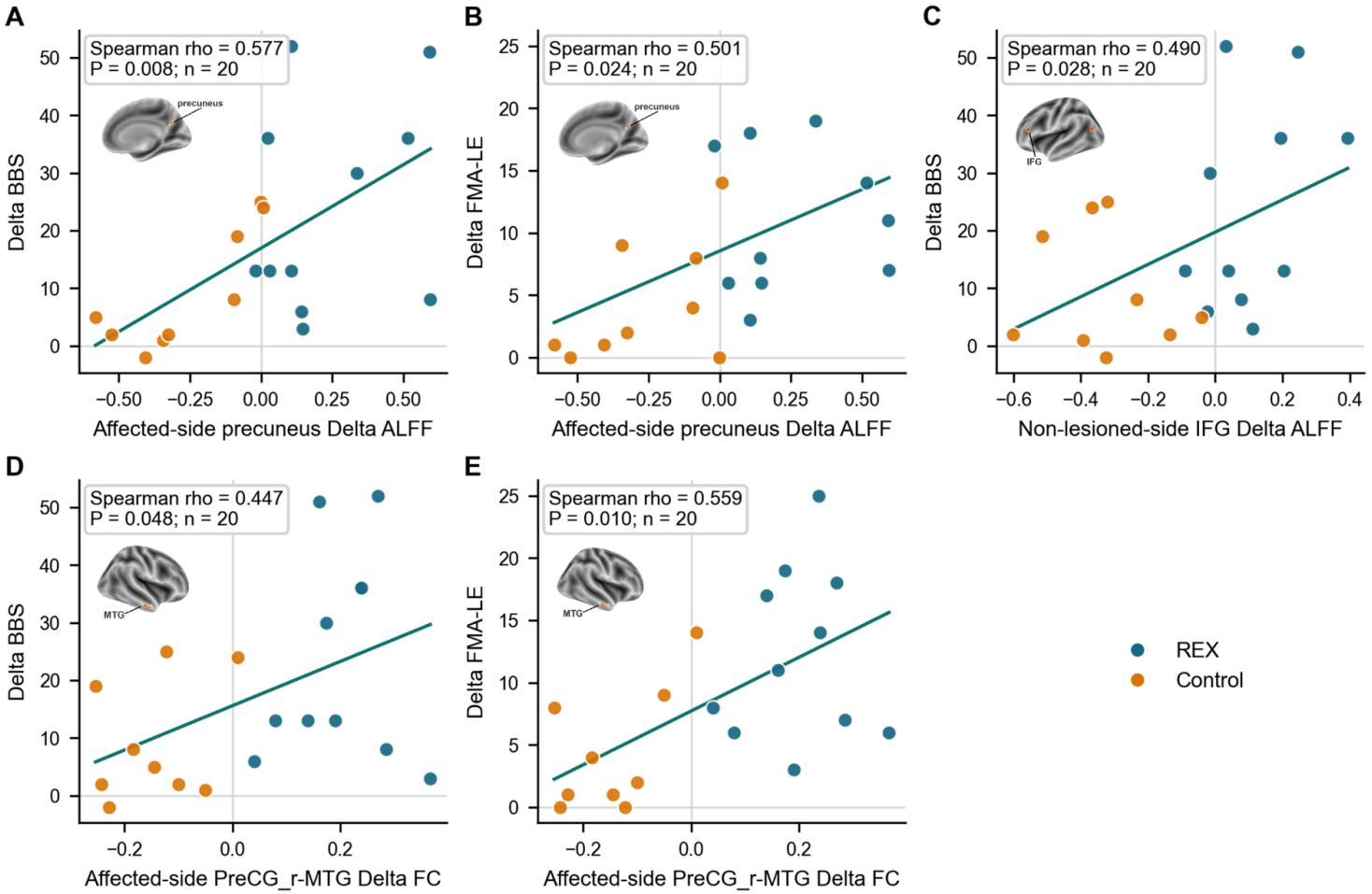
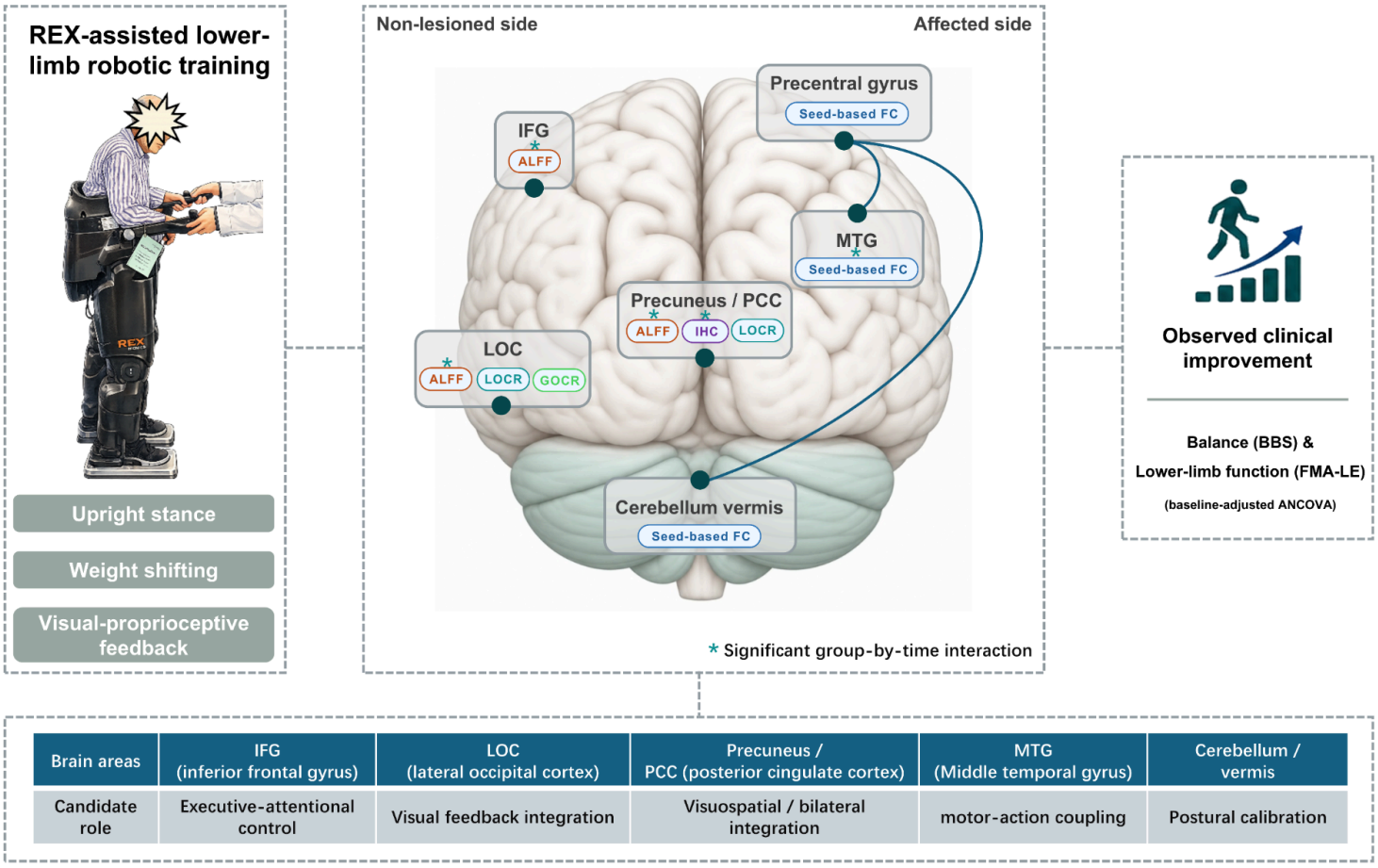


Figure 5

Exploratory pooled associations between formal rs-fMRI findings and clinical changes. Points are coloured by treatment group (REX, blue; control, orange), whereas Spearman correlations were calculated across all 20 imaging-retained participants. (A) Right precuneus ΔALFF versus ΔBBS; (B) right precuneus ΔALFF versus ΔFMA-LE; (C) left IFG ΔALFF versus ΔBBS; (D) PreCG_r–right MTG ΔFC versus ΔBBS; and (E) PreCG_r–right MTG ΔFC versus ΔFMA-LE. Lines are visual guides only. These pooled exploratory associations do not establish group-specific effects, mediation, or causality. Left, non-lesioned side; Right, affected side.



Brain areas	IFG (inferior frontal gyrus)	LOC (lateral occipital cortex)	Precuneus / PCC (posterior cingulate cortex)	MTG (Middle temporal gyrus)	Cerebellum / vermis
Candidate role	Executive-attentional control	Visual feedback integration	Visuospatial / bilateral integration	motor-action coupling	Postural calibration

Figure 6

Candidate framework summarizing REX-associated clinical and rs-fMRI observations. Asterisks indicate significant group-by-time interactions in the imaging subset (REX, n=11; control, n=9): ALFF in the IFG, LOC, and precuneus; IHC in bilaterally mirrored precuneus/PCC regions; and seed-based FC between the right precentral-gyrus (PreCG_r) seed and MTG. The cerebellum/vermis seed-based FC finding and the LCOR/GCOR observations represent exploratory within-REX pre-post changes and did not show significant group-by-time interactions. Candidate functional roles are hypothesis-generating, and lines indicate conceptual associations rather than neural directionality, mediation, or causality. Clinical improvement refers to favorable baseline-adjusted effects on BBS and FMA-LE in the full randomized sample. For display, left-lesion images were flipped so that the affected hemisphere is shown on the right. Thresholded fMRI maps used voxel-level $P < 0.001$, uncorrected, and cluster-level P-FDR < 0.05.

Supplementary Files

This is a list of supplementary files associated with this preprint. Click to download.

- supplementarymaterial.docx
- CONSORT2010Checklist.pdf